International Journal of Psychosocial Rehabilitation, Vol. 24, Issue 02, 2020
ISSN: 1475-7192

Structural Characterization of Magnesium-based Metal-organic Framework Carbon Composites

Khaliesah Kamal, Mohamad Azmi Bustam*, Azmi Mohd Shariff,
Pascaline Pré and Lomig Hamon

Abstract--- *A magnesium-based metal-organic framework (MOF), Mg-MOF-74, has been denoted as a landmark of its kind for CO2adsorption owing to its highly porous structure and strong metal adsorptive sites. However, large void spaces in the framework cannot be not fully utilized at ambient conditions due to weak surface dispersive forces. For that reason, two carbonaceous agents, multiwalled carbon nanotubes (CNT) and monolayer graphene oxide (GO), were used to enrich the formation of micropores in the original structure. The objective of the study is to characterize the structure of these new nanomaterials. Mg-MOF-74@CNT and Mg-MOF-74@GO composites were synthesized under solvothermal reaction and characterized by FESEM, EDXS, PXRD and FTIR analysis. Both GO and CNT were introduced into the framework via in-situ synthesis of 'bottle-around-ship' method to form homogeneous structure with MOF units. The insertion of composing materials was confirmed under FESEM morphological analysis. The profiles of PXRD and FTIR showed that the crystalline structure of Mg-MOF-74 was well preserved and not ruptured by the hybrid agents. Those structural analyses gave information on the nucleation of Mg-MOF-74 crystallites, increment of metal adsorptive sites, synergetic formation of CNT- and GO-MOF, crystallites size distribution, dilatation of crystallites and coordination of carboxylate ligands.*

Keywords--- *Adsorption, Carbon Dioxide, Metal-Organic Framework, Graphene Oxide, Carbon Nanotubes, Characterization.*

I. INTRODUCTION

As reported in International Energy Outlook 2016 forecast, natural gas is the fastest-growing primary energy resource with the projection to 2040[1]. Natural gas is a cleaner fuel in comparison to petroleum and coal making the world consumption increases to nearly double between 2001 and 2025[2]. Natural gas is favorable for the least greenhouse effects considering that the combustion emits lower quantities of CO_2 and other greenhouse gases. Although natural gas is relatively low in energy content per unit volume due to its gaseous state, it has the highest hydrogen content and higher energy conversion efficiencies for power generation comparatively to other hydrocarbon resources[3]. For efficiency reason, CO_2 which is the major impurity found in natural gas streams should be removed in order to produce a pure state of methane as the end-product. This undesired gas degrades the heating value of natural gas, reduces pipelines capacities, causes corrosion in distribution networks and contributes to global warming and climate changes [4].

Khaliesah Kamal, Department of Chemical Engineering, Universiti Teknologi PETRONAS, Teronoh, Malaysia.
Department of Environment and Energy Systems, GEPEA CNRS Unit, IMT Atlantique, Nantes, France.
Mohamad Azmi Bustam, Department of Chemical Engineering, Universiti Teknologi PETRONAS, Teronoh, Malaysia.*
E-mail: azmibustam@utp.edu.my
Azmi Mohd Shariff, Department of Chemical Engineering, Universiti Teknologi PETRONAS, Teronoh, Malaysia.
Pascaline Pré, Department of Environment and Energy Systems, GEPEA CNRS Unit, IMT Atlantique, Nantes, France.
Lomig Hamon, Department of Environment and Energy Systems, GEPEA CNRS Unit, IMT Atlantique, Nantes, France.

DOI: 10.37200/IJPR/V24I2/PR200540
Received: 26 Dec 2019 | Revised: 10 Jan 2020 | Accepted: 21 Jan 2020

The most renowned process, amine-based scrubbing, has been taking place for purifying natural gas for over 70 years, but it is uncertain if this technology is able to cater the scale of worldwide CO_2emitted which is 30 Giga tons per year[5]. Therefore, researches are continuously being conducted to either make improvement in the existing technologies or develop new effective materials to capture CO_2. The other techniques such as adsorption, membranes, cryogenic distillation, gas hydrates and chemical looping have been also taking place to mitigate CO_2 emissions aside from the traditional absorption[6]. Besides that, the use of solvents in absorption technique is controversial because of the corrosions of units, environmental hazards of their disposal and damages of pump suctions when the solvents vaporize[4]. Adsorption in which solid-state sorbents are used is viewed as a competitive technology for CO_2 removal with many potential advantages over absorption that uses solvents[7]. Among various technologies, adsorption is a strong candidate for CO_2/CH_4 separation owing to its high energy efficiency and low operating cost [8]with high purity of produced methane [4]. The most widely used CO_2adsorbents are zeolite, silica, alumina, activated carbon, graphene oxide and other carbon materials.

In the past decades, a new family of porous solid called metal-organic framework (MOF) has been the focus of intense research due to its unique properties for gas separation such as highly porous, tunable structure and adjustable functionalities[9]. MOF is recognized for their ability to provide immense specific surface area that cannot be achieved by other solid sorbents [10]. Other than their exceptional capacity, MOF also exhibits high thermal stability, large void volume and pore opening, facile synthesis, permanent and flexible porosity allowing the adaptation between pores size and the adsorbate, and, excellent selectivity by virtue of their tunable structures and adjustable functionalities[10-13]. Mg-MOF-74 has attracted the attention the most for its excellent balance between high dynamic capacity of CO_2adsorption and high CO_2/CH_4 separation selectivity. Mg-MOF-74 was claimed having one of the highest CO_2uptake capacities among other adsorbents in presence up to 8 mmol/g[14-16]. The ability to perform CO_2/CH_4 separation with an excellent thermodynamic selectivity was also proven. A breakthrough experiment showed that there was no CH_4 effluent concentration in Mg-MOF-74 before the saturation of CO_2[17]. The selectivity separation of CO_2/CH_4 in Mg-MOF-74 is as high as 330 which is among the best reported in MOF studies[17].

Although MOF displays the highest specific surface area in porous materials, it has a few feeble points by which its full potential in gas adsorption is hindered. Large void spaces within the framework could not be fully utilized by the reason of weak dispersive forces between pore walls and gaseous adsorbates[18-20]. MOF structure that is filled up with the void spaces is not favorable for the retention of small molecules at ambient conditions[21]. A number of structural modifications of the virgin MOF were proposed as strategies to enhance the uptake of CO_2. Recently, researches on the incorporation of MOF with carbon compounds from which MOF carbon composite (MCC) was produced were being conducted. MCC were reported able to increase the adsorption capacity of desired gas and enhance gas separation selectivity significantly more than their parent materials[18-37]. The embedment of carbonaceous agent in MOF void spaces leads to the formation of new micropores with an improved surface dispersive force [27]. As the result, the interaction between pore walls and the trapped $CO_2$was strengthened [38] since one-half of isosteric heat of adsorption is accounted for dispersion force [39].

DOI: 10.37200/IJPR/V24I2/PR200540
Received: 26 Dec 2019 | Revised: 10 Jan 2020 | Accepted: 21 Jan 2020

A higher retention of CO2 was achieved and consequently increased the selectivity of the adsorption which is the important factor in gas purification.

Motivated by the above thoughts, this particular research is prompted from the challenge of improving the adsorbing ability of the existing Mg-MOF-74 for selective separation of CO_2/CH_4. For that purpose, two carbonaceous hybrid agents, multiwalled carbon nanotubes (CNT) and monolayer graphene oxide (GO) were used as carbonaceous hybrid agents. The upgrading work highlighted is targeted to fulfil two conditions; enriching nanoporous structure of Mg-MOF-74 to increase its physical adsorption force (capacity) and improving adsorption chemistry within the framework to enable stronger retention towards CO_2 (selectivity). Therefore, this work will be the preliminary studies of these new materials before being applied in CO_2/CH_4 separation. The objective is firstly to produce Mg-MOF-74@CNT and Mg-MOF-74@GO composites using in-situ 'bottle-around-ship' synthesis under solvothermal reaction, secondly to study their structural characterization under FESEM, PXRD and FTIR analysis.

II. METHODOLOGY / MATERIALS

2.1 Synthesis

2.1.1 Synthesis of Mg-MOF-74

The following is the synthesis method improved from[16]. Soluble metal salt, $Mg(NO_3)_2.6H_2O$ (712 mg, 2.78 mmol) and 2,5-dihydroxyterephtalic acid linker (DOT) (167 mg, 0.84 mmol) were completely dissolved in dimethylformamide (DMF) (67.5 mL)/ethanol (4.5 mL)/H2O (4.5 mL) mixture under sonication for 15 minutes. The homogeneous solution was then transferred into a 125-mL Teflon lined stainless-steel autoclave reactor. The reactor was tightly capped and put in the oven at 125 °C to allow the reaction under autogenous pressure for 26 h. After that, the sample was removed and cooled at room temperature. The mother liquor of the reaction was gently separated from the product. The product was then washed using DMF and separated by centrifugal technique at 8000 rpm for 7 minutes. The same step of washing was repeated using methanol for 3 times. The product was then immersed in methanol in a Petri dish to remove solvents that still blocked the pores. The methanol was replenished with fresh methanol 6 times for 3 days. The product was again separated from the methanol by using centrifuge. The wet powder was dried under mild temperature in the oven before the solvent was evacuated under a dynamic vacuum at 250 °C for 15 h. Mg-MOF-74 was labelled as M.

2.1.2 Synthesis of Mg-MOF-74@GO and Mg-MOF-74@CNT composites

The composites were synthesized by using the same method as presented previously except the composing material was included before the sonication by direct mixing as reported elsewhere [19-23]. The composing materials adopted were CNT (multiwalled >7.5% basis, 7-15 nm diameter, 0.5-10 µm length, >99% purity) and GO (monolayer content >95%, oxygen content ≥36%, 4 mg/mL dispersion in H_2O). Both Mg-MOF-74 reagents and composing material took part from the beginning of the reaction to form homogeneous structure of GO- or CNT-frameworks. This method was referred to in-situ synthesis of ‘bottle-around-ship’ (BAS) method in which the composing materials intercalate within the cage of MOF units [38]. The sonication was carried out for 2 h to make sure the composing material was completely dissolved. CNT powder and GO dispersion in 4 mg/mL H_2O were

DOI: 10.37200/IJPR/V24I2/PR200540
Received: 26 Dec 2019 | Revised: 10 Jan 2020 | Accepted: 21 Jan 2020

measured in mass-basis to obtain 0.3 wt% by referring to the weight of the parent Mg-MOF-74 produced in the previous synthesis. The composites were denoted as MG for Mg-MOF-74@GO and MC for Mg-MOF-74@CNT.

2.1.3 Extraction of GO from water dispersion

Since GO used in the synthesis was commercially provided in water dispersion, the extraction of GO was necessary to study its properties and behavior to be compared with the composite. For that purpose, 100 mL of 4 mg/mL GO solution was dissolved in 260 mL of acetone and stirred to obtain precipitation. The solution was then poured into six centrifuge tubes for 30 mL each for GO separation. The centrifugation speed and time were fixed respectively 7000 rpm and 30 minutes. The sediment of wet GO solid was collected and dried in the oven at 80 °C overnight. As the product, GO flakes were obtained.

2.2 Characterization

2.2.1 FESEM analysis

Zeiss SUPRA 55VP instrument was used to study the morphology, porous structure and particle size of the samples. The micrographs were visualized from 1k to 100k of magnification. Energy dispersive x-ray spectroscopy (EDXS) analysis was also carried out to analyze the contain of the elements on the surface of the samples.

2.2.2 PXRD analysis

The crystalline structure of the samples was confirmed by using powder X-ray diffraction. XRD patterns were recorded by using Bruker AXS D8 Advance Diffractometer with Cu Kα radiation (λ= 1.5406 Å), a step size of 0.02° in 2θranged from 5° to 50°, an exposure time of 100 s/step and a scan rate of 0.1 °/min.

2.2.3 FTIR analysis

FTIR spectrum was recorded by using Nicolet 400D Shimadzu Spectrometer in the region of 4000-500 cm^{-1}.

III. RESULTS AND FINDINGS

3.1 Synthesis

As the product, Mg-MOF-74 powder was obtained in light yellow color while Mg-MOF-74@CNT and Mg-MOF-74@GO were in form of greenish yellow powder. Approximately 200 mg of the final sample was produced in one-batch of reaction whereby the composites were produced slightly higher in amount relatively to Mg-MOF-74. A basic calculation showed that the yield of production reached 85%. Almost 400 mg of non-reactive components was removed during washing process.In another synthesis using microwave-heating method, the pressure of the reaction was observed approximately 40 bar. The density of the samples was estimated 0.18 g/cm^3.

Theoretical: **2.78** $[Mg(NO_3)_2.6H_2O]$ + **0.84** $[C_8H_6O_6]$ $\rightarrow$ **0.93** $[Mg_3O_3(CO_2)_3]$ + others

Experimental: **2.78** $[Mg(NO_3)_2.6H_2O]$ + **0.84** $[C_8H_6O_6]$ $\rightarrow$ **0.79** $[Mg_3O_3(CO_2)_3]$ + others

3.2 FESEM analysis

The morphology of Mg-MOF-74, Mg-MOF-74@CNT and Mg-MOF-74@GO are shown in Figure 1-Figure**5**. All samples exhibited irregular sizes of hexagonal cylindrical shape which referred to the original crystal of Mg-

DOI: 10.37200/IJPR/V24I2/PR200540
Received: 26 Dec 2019 | Revised: 10 Jan 2020 | Accepted: 21 Jan 2020

MOF-74 (Figure 1a). However, crystal size distribution (CSD) of single nucleation in the samples was notably different; MOF crystallites grew a bit larger with the addition of CNT and much larger with GO. CDS estimation showed that the samples displayed very wide population of particle sizes (diameters) from 0.05-10 μm in a-axis direction. Single crystalline specimen with maximum dimensions of Mg-MOF-74 (Figure 1b), Mg-MOF-74@CNT (Figure 1c) and Mg-MOF-74@GO (Figure 1d) were captured under SEM with diameters and heights presented in Table 1. The cross-sectional image of Mg-MOF-74 showed that the adsorbent was full with highly nanoporous framework (Figure 2a,b). In both composites, it was noticed that the secondary nucleation of MOF units was preferable than the primary growth. By the presence of the composing materials, free energy formation of nanocrystallites decreased with the disturbance in space leading to an increased number of crystallite nucleation sites, rather than the growth of the existing crystallites. As the result, a larger crystal volume was produced with smaller crystallite sizes. The similar observation was deduced by Nutor (2018) [40] in the study of the effect of tensile stress annealing on alloy's nucleation. In Mg-MOF-74@CNT, some platelets were found randomly agglomerated due to cross-binding of CNT through in-and-out of the framework interlocked with the bridging ligands (Figure 3a).

The substitution of CNT has occurred along with the reaction of Mg-BDC which made them embedded homogeneously with the framework (Figure 3b,c). The average diameter of the inserted CNT was estimated close to 17 nm which was in accordance with manufacturer's specification (Figure 3d). In Mg-MOF-74@GO, some platelets tended to form chorales of crystallites (Figure 4a) of which the edges were interchained each other by intercalation of GO layers between hexagonal corners of the crystallites (Figure 4b). The attachment of GO layers at their edges was observed as in (Figure 4c,d) causing their architecture became less sharp. The development of crystallites in the choral might be hindered by these walls and that explained the nano-sized units produced in the chorale. Besides that, the presence of GO also lead to a layer-by-layer sandwiched structure of MOF units/GO layers (Figure 5a,b). These heterostructures occurred when GO layers lied alternately between the bodies of the crystallites as visualized in Fig. 6. Two hypotheses of the synergy between Mg-MOF-74 and GO can be deduced; 1) the growth of some crystals took place on the layers of GO, and, 2) oxygen-functional groups in GO reacted with Mg-sites, both of which gave raise to homo- and hetero-formation of polycrystalline MOF and GO. In earlier studies, the reaction of O atoms of GO with copper sites of octahedral HKUST-1 was mentioned by Zhao (2014) and Petit (2011b) [20, 33]. EDXS analysis on the surface of the substrate indicated that there was not big difference in the elements composition as presented in Table 1.

The insignificant percentage of substitution of CNT and GO was the reason why C and O atoms were found much less in all samples. It was the atoms of organic linkers that contributed the most. However, a small addition of Mg atoms was detected in both composites proving that the metal adsorptive sites could be enriched by CNT and GO insertion. Due to Mg increment, the atomic percentage of O was also increased owing to polyhedral coordination units of MgO_5. To have a bigger picture on the incorporation chemistry between Mg-MOF-74 and carbon composing materials, HRTEM analysis is suggested for a deeper insight.

DOI: 10.37200/IJPR/V24I2/PR200540
Received: 26 Dec 2019 | Revised: 10 Jan 2020 | Accepted: 21 Jan 2020

ISSN: 1475-7192

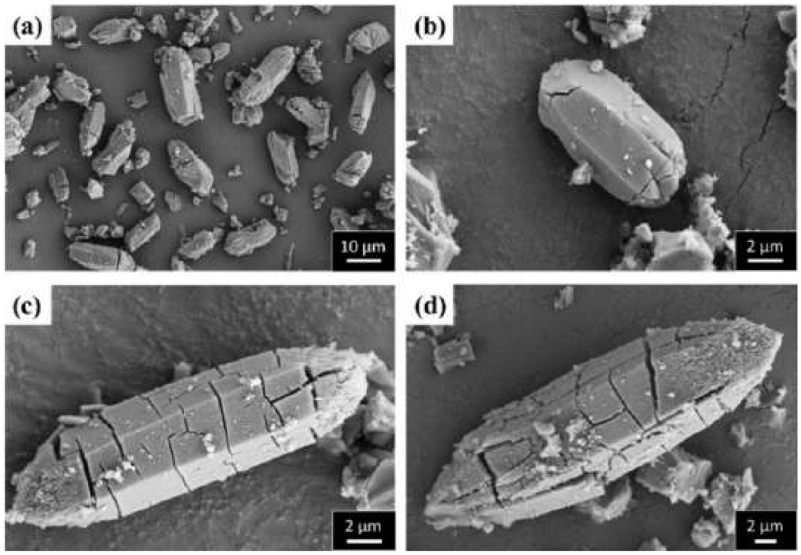

Figure 1: FESEM micrographs of (a) Mg-MOF-74 view from above, and, single crystallite with maximum dimensions of (b) Mg-MOF-74, (c) Mg-MOF-74@CNT and (d)Mg-MOF-74@GO.

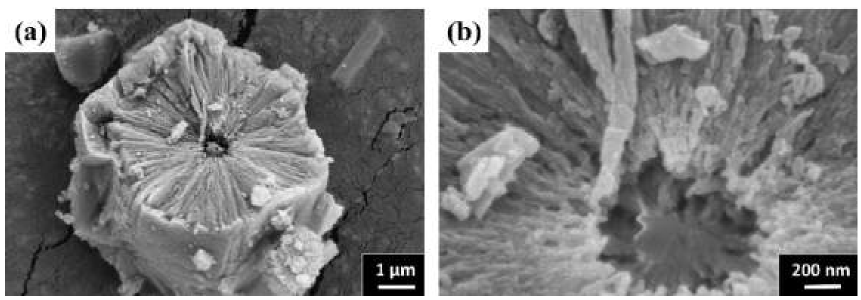

Figure 2: FESEM micrographs of cross-section of Mg-MOF-74.

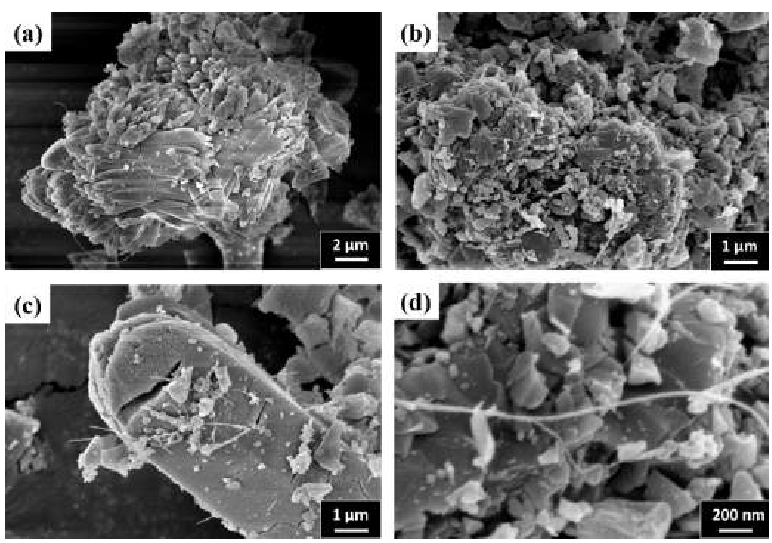

Figure 3: FESEM micrograph of Mg-MOF-74@CNT; (a) agglomeration of MOF crystallites, (b)-(c) homogeneous formation of MOF-CNT, and, (d) inserted CNT

DOI: 10.37200/IJPR/V24I2/PR200540
Received: 26 Dec 2019 | Revised: 10 Jan 2020 | Accepted: 21 Jan 2020

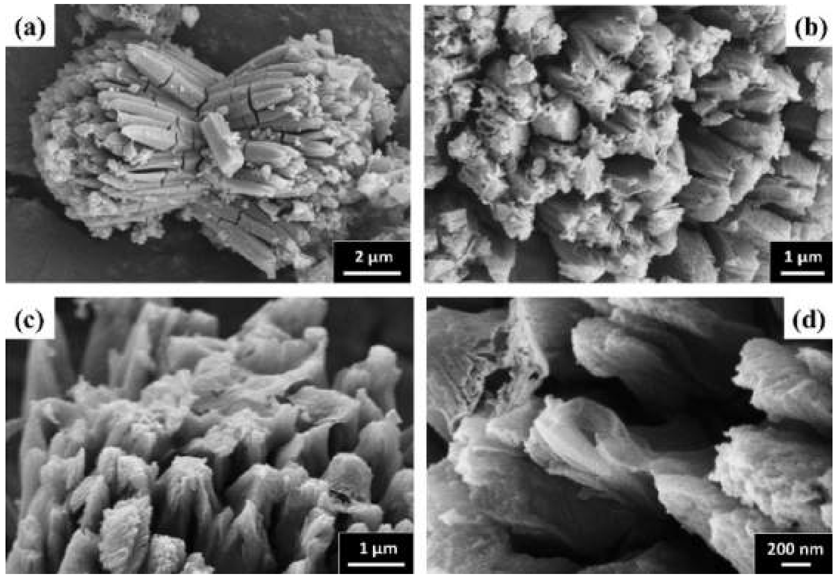

Figure 4: FESEM micrograph of Mg-MOF-74@GO; (a) chorale of MOF crystallites, (b) interchained edges, (c)-(d) GO attachment.

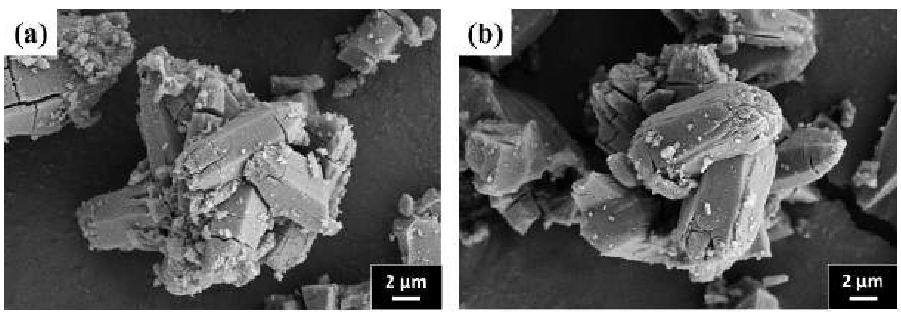

Figure 5: FESEM micrographs of layer-to-layer sandwiched structure of MOF crystallites/GO layers in Mg-MOF-74@GO

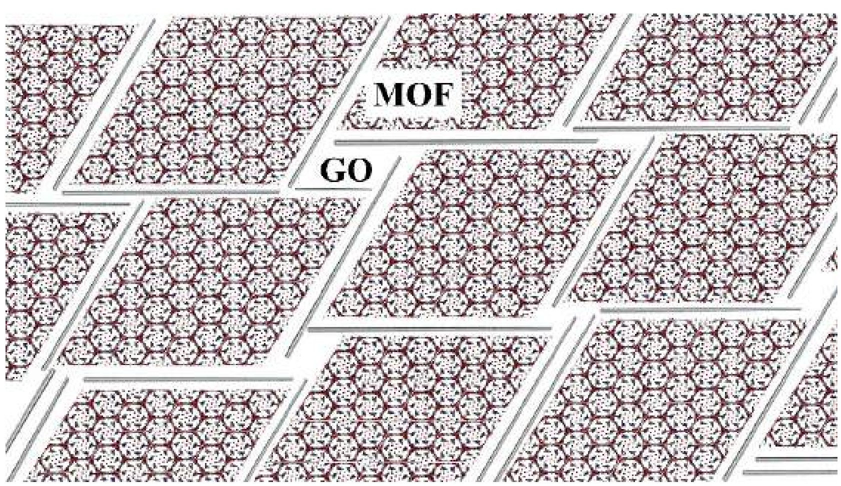

Figure 6: Visualization of MOF-GO formation in Mg-MOF-74@GO

DOI: 10.37200/IJPR/V24I2/PR200540
Received: 26 Dec 2019 | Revised: 10 Jan 2020 | Accepted: 21 Jan 2020

Table 1: Maximum crystallite size and EDXS analysis of Mg-MOF-74, Mg-MOF-74@CNT and Mg-MOF-74@GO.

Samples	**Crystallite dimensions (μm)**		**EDXS analysis (% atomic)**		
	Diameters	**Height**	**Mg**	**O**	**C**
M	5	10	13.88	42.5	43.62
MC	6	23	14.27	49.68	36.05
MG	10	37	15.8	47.6	36.59

3.3 PXRD analysis

Figure 7shows that all samples exhibited sharp characteristic peaks at 6.9°, 11.9°, 13.7°, 15.3°, 16.8°, 18.1°, 19.4°,20.5°, 21.7°, 23.8°, 24.7°, 25.7°, 26.6°, 27.5°, 28.4°, 29.2°, 30.0°, 30.8°, 31.6°, 33.8° and 34.5° which were in perfect agreement with powder diffraction pattern calculated using Material Studio modelling. This showed that those composites had good crystallinity as same as Mg-MOF-74. The original structure was well preserved indicating that the formation of Mg-BDC was not retarded by the composing materials. However, the presence of CNT and GO could not be detected in this analysis. They respectively exhibited diffraction peaks at 11.9° and 26.1° which were the same appeared in Mg-MOF-74 pattern. Since they were substituted with a very small percentage, their peaks were difficult to be distinguished with MOF's. Other reason related to this result was the dispersion of CNT and GO within MOF units that made them not visible in XRD profiles. The highest peaks were observed at 6.9° and 11.9° demonstrated the highest number of diffracting particles in (110) and (300) planes. Those planes which represented Miller indices (hkl) were determined by plane-spacing equation and Bragg's law equation and agreed well with reported elsewhere [41, 42]. However, a hexagonal closed-pack (HCP) unit was comprised of 4 directions of vertical c-axis which was perpendicular to basal plane and horizontal $a_{(1-3)}$-axis that lied on the basal plane (Figure 9a). Therefore, the planes in HCP were designated by 4-index Miller-Bravais notation (hk i l) where i =-(h+k). It was eventually deduced that (11 -20) prismatic plane and (30 -30) plane as shown in (Figure 9b) were respectively dedicated to 6.9° and 11.9°. A zoom-in image in Figure 8focused on diminished intensity of the highest peaks of Mg-MOF-74@CNT and Mg-MOF-74@GO which also happened for all characteristic peaks. The reduction did not present the degradation in crystallinity degree of the lattices, yet it was an indicative to concentration vacancies of electron density in the unit cell. Knowing that diffracting peaks of MgO occurred at high scattering angles and supporting by EDXS result, the vacancies might be related to decreased diffracting C atoms in the composites. Besides that, it was also remarked that the peaks of Mg-MOF-74@GO slightly displaced to lower scattering angle with an important difference of 0.25°. There were many possible reasons that contributed to this systematic shifting of all 2θvalues such as sample displacement, zero drift from XRD equipment or temperature. A standard reference material was run to correct the displacement error to the position defined by the standard peak. The measurement of Mg-MOF-74 was repeated and it came out with the same shifted profiles. A hypothesis that can be deduced was the expansion of the lattices in c-axis direction due to strain contribution. The structural relaxation of the lattice was driven by the substitution of oversized GO into the framework. The same distortion of lattices was also figured out byYabuuchi (2014)[43] when doping gadolinium into gallium nitride films. Our result was then supported by the calculation of average crystallite sizes using Scherrer's equation in which Mg-MOF-74@GO was proven having larger crystallite than Mg-MOF-74 and Mg-MOF-74@CNT (Table 2).

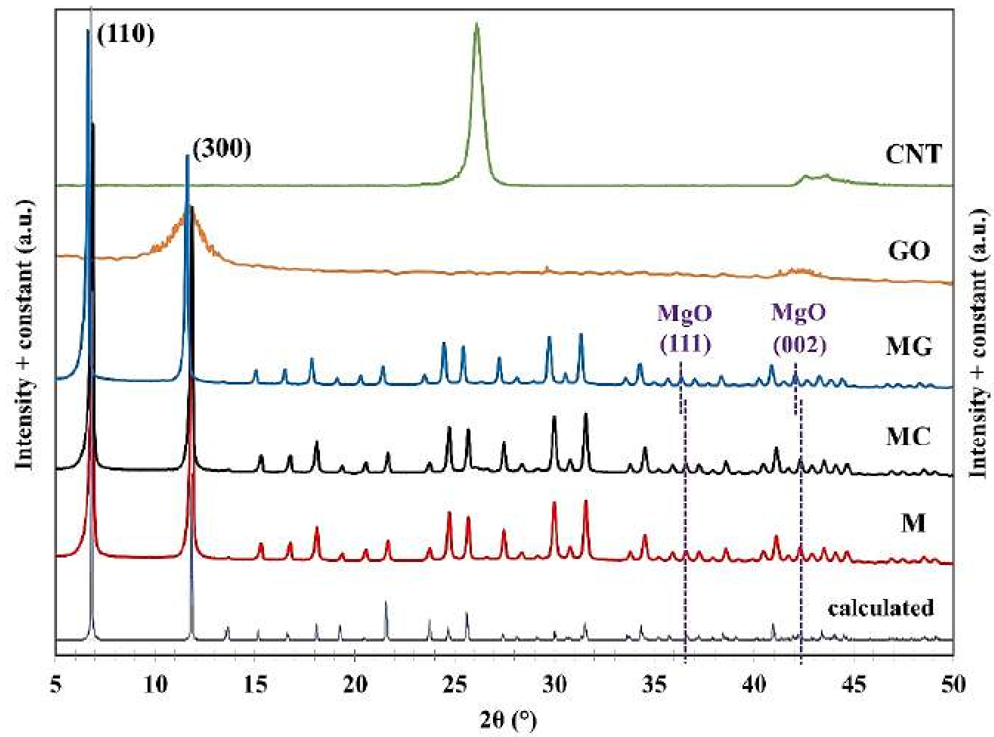

Figure 7: PXRD profiles ofMg-MOF-74, Mg-MOF-74@CNT, Mg-MOF-74@GO in primary axis, and, CNT, GO in secondary axis

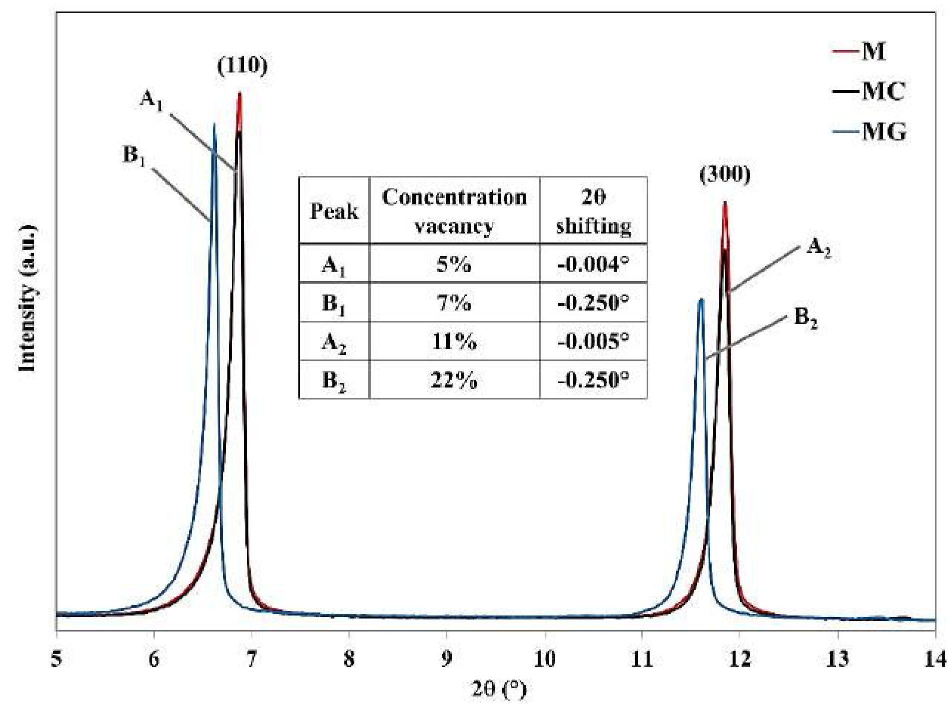

Figure 8: Significant peaks of Mg-MOF-74, Mg-MOF-74@CNT and Mg-MOF-74@GO

DOI: 10.37200/IJPR/V24I2/PR200540
Received: 26 Dec 2019 | Revised: 10 Jan 2020 | Accepted: 21 Jan 2020

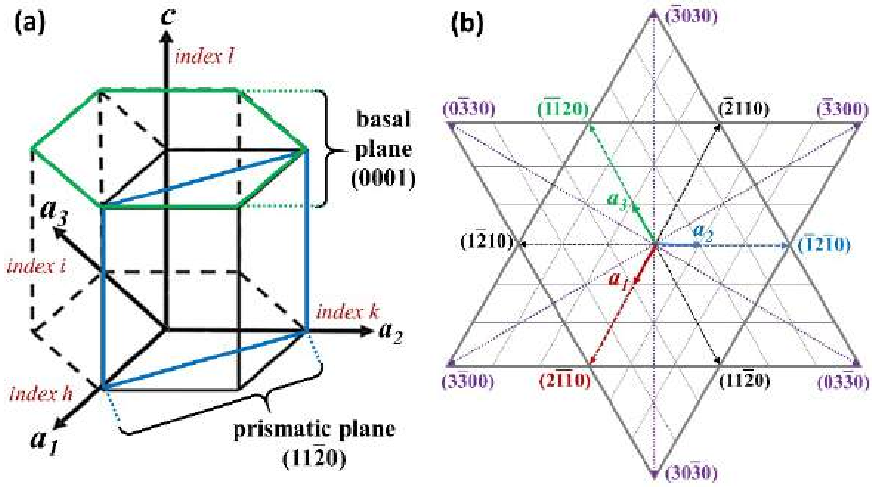

Figure 9: Directions and planes of hexagonal close-packed structure indicated by Miller-Bravais indices.

Table 2: Average crystallite sizes calculated using Scherrer's equation.

Samples	Angle (°)	FWHM (°)	Crystallite diameters (nm)
M	6.87	0.1023	73.3 ± 11.3
	11.85	0.1023	
MC	6.87	0.1023	73.3 ± 11.3
	11.85	0.1023	
MG	6.62	0.1023	81.5 ± 0.2
	11.6	0.1279	

3.4 FTIR analysis

Figure 10 shows that IR spectral bands of Mg-MOF-74 and the composites nearly as same as 2,5-dihydroxyterephtalic acid (DOT) used in the synthesis. However, the carboxylate-based linker exhibited a broader O-H stretching band in 3700-2340 cm^{-1}(region A) and stronger C-H alkane stretching vibrations between 3200 and 2500 cm^{-1}(region B). Both O-H and C-H stretching bands progressively faded during the formation of MOFs. A miniscule peak at 1760 cm^{-1}(point C) was situated in carbonyl region (1840-1740 cm^{-1}) indicating the presence of anhydrides (-CO-O-CO-) before the reaction. Marked with red lines, symmetric stretching vibrations of carboxylate groups in Mg-MOF-74, Mg-MOF-74@CNT and Mg-MOF-74@GO shifted to 1590 $cm^{-1}$from a lower wave number in DOT, 1650 cm^{-1}. A significant peak in DOT at 1500 $cm^{-1}$was referred to the aromatic stretching band and it almost disappeared in MOFs spectra. All peaks appeared in 1370-1000 cm^{-1}(region D) signified in-plane C-H bending whereas in the lower wave number range (1000-500 cm^{-1}, region E) indicated out-of-plane C-H bending [44]. Meanwhile, asymmetric stretching of carboxylate groups in DOT and all samples was observed at 1430 cm^{-1},marked with blue line. Those asymmetric peaks remained visible in MOFs spectra but with a slight shifting and significant reduced intensity. In order to study the coordination of carboxylate groups with metal sites, the separation value between the symmetric and asymmetric peaks was calculated, $\Delta = \lambda_{SYM}(COO^-) - \lambda_{ASSYM}(COO^-)$ [45]. For Δ>200 $cm^{-1}$and Δ<110 cm^{-1}, monodentate and bidentate ligands were respectively expected, while Δ in the range of 138-200 cm^{-1}represented a bridging ligand. The calculated value of Δ (DOT) was 220 whereas Δ(Mg-MOF-74, Mg-MOF-74@CNT, Mg-MOF-74@GO) was 160. Therefore, it was concluded that carboxylate groups in DOT

DOI: 10.37200/IJPR/V24I2/PR200540
Received: 26 Dec 2019 | Revised: 10 Jan 2020 | Accepted: 21 Jan 2020

existed in form of monodentate ligand. In MOFs, the carboxylate groups were deduced binding with metal cations to form bridging ligands of the framework.

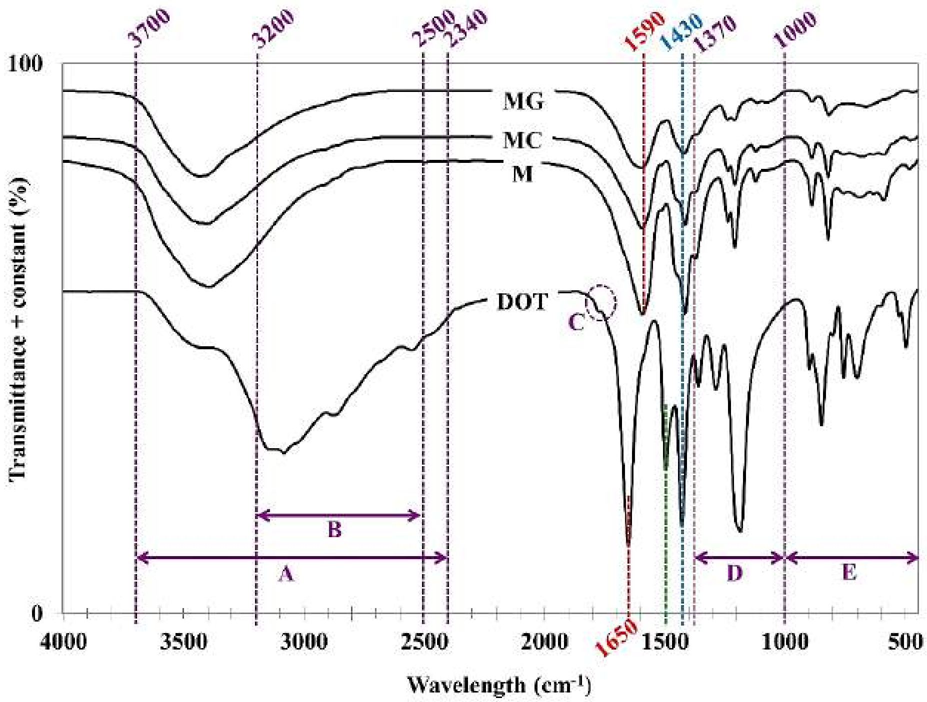

Figure 10: FTIR spectra of DOT linker, Mg-MOF-74, Mg-MOF-74@CNT and Mg-MOF-74@GO

IV. CONCLUSION

Mg-MOF-74@CNT and Mg-MOF-74@GO were successfully synthesized under solvothermal reaction at 0.3 wt% of substitution. The formation of the composites was considered as homogeneous. The presence of CNT promoted agglomeration of Mg-MOF-74 crystallites during their nucleation due to interlocking of nano-tube structure with bridging ligands of Mg-MOF-74. XRD and FTIR profiles of Mg-MOF-74@CNT showed that the composite had almost similar characteristic to the pristine MOF, indicating that CNT did not bring much difference in nanostructural modification. However, the adsorptive metal sites were profitably enriched by CNT and GO addition. The embedding of GO popularized multinucleation of Mg-MOF-74 lattices in form a choral leading to increased crystal volume with decreased crystallite sizes. Under SEM and XRD analysis, the single nucleation of Mg-MOF-74@GO was observed larger in size when compared to Mg-MOF-74 and Mg-MOF-74@CNT. The elongation of the lattices in c-axis direction was expected due to interruption of oversized GO layers through the reaction of Mg-sites and oxygen-functional groups in GO. GO layers were also able to generate heteroformation of layer-by-layer sandwiched structure with Mg-MOF-74 units. Based on the result, the incorporation of Mg-MOF-74/CNT and Mg-MOF-74/GO were believed able to enhance microporous structure of the pristine MOF. The analysis of N_2 adsorption/desorption isotherm is indispensable to characterize specific surface areas, pores volume and pores size distribution.

DOI: 10.37200/IJPR/V24I2/PR200540
Received: 26 Dec 2019 | Revised: 10 Jan 2020 | Accepted: 21 Jan 2020

ACKNOWLEDGEMENT

This work is supported by URIF (project no. 0153AA-B90), YUTP (0153AA-H42) and PRGS (0153ABL46). The project is a collaborative research between Universiti Teknologi PETRONAS and GEPEA CNRS Unit, IMT Atlantique, Department of Environment and Energy Systems, 44307 Nantes, France.

REFERENCES

[1] EIA, "INTERNATIONAL ENERGY OUTLOOK 2016," United States Energy Information Administration, Forrestal Building, Washington, DC, ReportMay 2016 2016.

[2] A. Demirbas, "CHAPTER 2: NATURAL GAS," in *Methane Gas Hydrate*, ed: Springer New York, Science & Business Media, 2010, pp. 57-76.

[3] M. J. Economides and D. Wood, "THE STATE OF NATURAL GAS," *Journal of Natural Gas Science and Engineering*, vol. Vol. 1, pp. 1-13, 2009.

[4] S. Biruh and H. Mukhtar, "NATURAL GAS PURIFICATION TECHNOLOGIES-MAJOR ADVANCES FOR CO_2 SEPARATION AND FUTURE DIRECTIONS," in *Advance in Natural Gas Technology*, D. H. Al-Megren, Ed., ed Universiti Teknologi Petronas: INTECH 2012.

[5] J. Wilcox, "CHAPTER 1 : INTRODUCTION TO CARBON CAPTURE," in *Carbon Capture*, ed Department of Energy Resources Engineering, Stanford University: Springer New York, 2012.

[6] IPPC, "CHAPTER 3: CAPTURE OF CO_2," in *Special Report: Carbon dioxide Capture and Storage*, B. Metz, O. Davidson, H. C. De Coninck, M. Loos, and L. A. Meyer, Ed., ed Cambridge University Press, UK and NY USA Intergovernmental Panel on Climate Change, 2005, pp. 105-178.

[7] S. Faramawy, T. Zaki, and A.-E. Sakr, "NATURAL GAS ORIGIN, COMPOSITION, AND PROCESSING: A REVIEW," *Journal of Natural Gas Science and Engineering*, vol. 34, pp. 34-54, 2016.

[8] W. Huang, X. Zhou, Q. Xia, J. Peng, H. Wang, and Z. Li, "PREPARATION AND ADSORPTION PERFORMANCE OF GrO@Cu-BTC FOR SEPARATION OF CO_2/CH_4," *Industrial & Engineering Chemistry Research*, vol. 53, pp. 11176-11184, 2014.

[9] C. Dey, T. Kundu, B. P. Biswal, A. Mallick, and R. Banerjee, "CRYSTALLINE METAL-ORGANIC FRAMEWORKS (MOFS): SYNTHESIS, STRUCTURE AND FUNCTION," *Acta Crystallographica Section B: Structural Science, Crystal Engineering And Materials*, vol. 70, pp. 3-10, 2014.

[10] M. Hu, "DESIGN, SYNTHESIS AND APPLICATIONS OF METAL ORGANIC FRAMEWORKS," *Worcester Polytechnic Institute*, 2011.

[11] E. Ahmed, A. Deep, E. E. Kwon, R. J. Brown, and K.-H. Kim, "PERFORMANCE COMPARISON OF MOF AND OTHER SORBENT MATERIALS IN REMOVING KEY ODORANTS EMITTED FROM PIGPEN SLURRY," *Scientific Reports*, vol. 6, 2016.

[12] P. Horcajada, R. Gref, T. Baati, P. K. Allan, G. Maurin, P. Couvreur, *et al.*, "METAL–ORGANIC FRAMEWORKS IN BIOMEDICINE," *Chemical Reviews*, vol. 112, pp. 1232-1268, 2011.

[13] N. A. Khan, Z. Hasan, and S. H. Jhung, "ADSORPTIVE REMOVAL OF HAZARDOUS MATERIALS USING METAL-ORGANIC FRAMEWORKS (MOFs): A REVIEW," *Journal Of Hazardous Materials*, vol. 244, pp. 444-456, 2013.

[14] S. R. Caskey, A. G. Wong-Foy, and A. J. Matzger, "DRAMATIC TUNING OF CARBON DIOXIDE UPTAKE VIA METAL SUBSTITUTION IN A COORDINATION POLYMER WITH CYLINDRICAL PORES," *Journal of the American Chemical Society*, vol. 130, pp. 10870-10871, 2008.

[15] A. O. z. r. Yazaydın, R. Q. Snurr, T.-H. Park, K. Koh, J. Liu, M. D. LeVan, *et al.*, "SCREENING OF METAL−ORGANIC FRAMEWORKS FOR CARBON DIOXIDE CAPTURE FROM FLUE GAS USING A COMBINED EXPERIMENTAL AND MODELING APPROACH," *Journal of the American Chemical Society*, vol. 131, pp. 18198-18199, 2009.

[16] Z. Bao, L. Yu, Q. Ren, X. Lu, and S. Deng, "ADSORPTION OF CO_2 AND CH_4 ON A MAGNESIUM-BASED METAL ORGANIC FRAMEWORK," *Journal of Colloid and Interface Science*, vol. 353, pp. 549-556, 2011.

[17] D. Britt, H. Furukawa, B. Wang, T. G. Glover, and O. M. Yaghi, "HIGHLY EFFICIENT SEPARATION OF CARBON DIOXIDE BY A METAL-ORGANIC FRAMEWORK REPLETE WITH OPEN METAL SITES," *Proceedings of the National Academy of Sciences*, vol. 106, pp. 20637-20640, 2009.

[18] C. Petit, B. Levasseur, B. Mendoza, and T. J. Bandosz, "REACTIVE ADSORPTION OF ACIDIC GASES ON MOF/GRAPHITE OXIDE COMPOSITES," *Journal of Microporous and Mesoporous Materials,* vol. 154, pp. 107-112, 2012.

[19] Y. Chen, D. Lv, J. Wub, J. Xiao, H. Xi, Q. Xia, *et al.*, "A NEW MOF-505@GO COMPOSITE WITH HIGH SELECTIVITY FOR CO_2/CH_4 AND CO_2/N_2 SEPARATION," *Chemical Engineering Journal,* pp. 1065-1072, 2017.

[20] Y. Zhao, Y. Cao, and Q. Zhong, "CO_2 CAPTURE ON METAL-ORGANIC FRAMEWORK AND GRAPHENE OXIDE COMPOSITE USING A HIGH-PRESSURE STATIC ADSORPTION APPARATUS," *Journal of Clean Energy Technologies,* vol. 2, pp. 34-37, 2014.

[21] C. Petit, B. Mendoza, and T. J. Bandosz, "HYDROGEN SULFIDE ADSORPTION ON MOFS AND MOF/GRAPHITE OXIDE COMPOSITES," *Journal of ChemPhysChem*, vol. 11, pp. 3678-3684, 2010.

[22] X. Sun, Q. Xia, Z. Zhao, Y. Li, and Z. Li, "SYNTHESIS AND ADSORPTION PERFORMANCE OF MIL-101(Cr)/GRAPHITE OXIDE COMPOSITES WITH HIGH CAPACITIES OF n-HEXANE," *Chemical Engineering Journal*, vol. 239, pp. 226-232, 2014.

[23] S. J. Yang, J. Y. Choi, H. K. Chae, J. H. Cho, K. S. Nahm, and C. R. Park, "PREPARATION AND ENHANCED HYDROSTABILITY AND HYDROGEN STORAGE CAPACITY OF CNT@MOF-5 HYBRID COMPOSITE," *Chemistry of Materials Journal,* vol. 21, pp. 1893-1897, 2009.

[24] A. K. Adhikari and K.-S. Lin, "IMPROVING CO_2 ADSORPTION CAPACITIES AND CO_2/N_2 SEPARATION EFFICIENCIES OF MOF-74 (Ni,Co) BY DOPING PALLADIUM-CONTAINING ACTIVATED CARBON," *Chemical Engineering Journal,* vol. 284, pp. 1348-1360, 2016.

[25] M. Anbia and V. Hoseini, "DEVELOPMENT OF MWCNT@ MIL-101 HYBRID COMPOSITE WITH ENHANCED ADSORPTION CAPACITY FOR CARBON DIOXIDE," *Chemical Engineering Journal,* vol. 191, pp. 326-330, 2012.

[26] H. Askari, M. Ghaedi, K. Dashtian, and M. H. A. Azghandi, "RAPID AND HIGH-CAPACITY ULTRASONIC ASSISTED ADSORPTION OF TERNARY TOXIC ANIONIC DYES ONTO MOF-5-ACTIVATED CARBON: ARTIFICIAL NEURAL NETWORKS, PARTIAL LEAST SQUARES, DESIRABILITY FUNCTION AND ISOTHERM AND KINETIC STUDY," *Journal of Ultrasonics Sonochemistry,* vol. 37, pp. 71-82, 2017.

[27] V. Jabbari, J. Veleta, M. Zarei-Chaleshtori, J. Gardea-Torresdey, and D. Villagrán, "GREEN SYNTHESIS OF MAGNETIC MOF@GO AND MOF@CNT HYBRID NANOCOMPOSITES WITH HIGH ADSORPTION CAPACITY TOWARDS ORGANIC POLLUTANTS," *Chemical Engineering Journal,* vol. 304, pp. 774-783, 2016.

[28] B. Levasseur, C. Petit, and T. J. Bandosz, "REACTIVE ADSORPTION OF NO_2 ON COPPER-BASED METAL− ORGANIC FRAMEWORK AND GRAPHITE OXIDE/METAL−ORGANIC FRAMEWORK COMPOSITES," *ACS Applied Materials & Interfaces,* vol. 2, pp. 3606-3613, 2010.

[29] C. Petit and T. J. Bandosz, "ENHANCED ADSORPTION OF AMMONIA ON METAL-ORGANIC FRAMEWORK/GRAPHITE OXIDE COMPOSITES: ANALYSIS OF SURFACE INTERACTIONS," *Journal of Advanced Functional Materials,* vol. 20, pp. 111-118, 2010.

[30] C. Petit and T. J. Bandosz, "EXPLORING THE COORDINATION CHEMISTRY OF MOF–GRAPHITE OXIDE COMPOSITES AND THEIR APPLICATIONS AS ADSORBENTS," *Journal of Dalton Transactions,* vol. 41, pp. 4027-4035, 2012.

[31] C. Petit and T. J. Bandosz, "SYNTHESIS, CHARACTERIZATION, AND AMMONIA ADSORPTION PROPERTIES OF MESOPOROUS METAL–ORGANIC FRAMEWORK (MIL (FE))–GRAPHITE OXIDE COMPOSITES: EXPLORING THE LIMITS OF MATERIALS FABRICATION," *Journal of Advanced Functional Materials,* vol. 21, pp. 2108-2117, 2011.

[32] C. Petit and T. J. Bandosz, "MOF–GRAPHITE OXIDE COMPOSITES: COMBINING THE UNIQUENESS OF GRAPHENE LAYERS AND METAL–ORGANIC FRAMEWORKS," *Journal of Advanced Materials,* vol. 21, pp. 4753-4757, 2009.

[33] C. Petit, J. Burress, and T. J. Bandosz, "THE SYNTHESIS AND CHARACTERIZATION OF COPPER-BASED METAL–ORGANIC FRAMEWORK/GRAPHITE OXIDE COMPOSITES," *Journal of Carbon,* vol. 49, pp. 563-572, 2011.

[34] C. Petit, B. Mendoza, and T. J. Bandosz, "REACTIVE ADSORPTION OF AMMONIA ON Cu-BASED MOF/GRAPHENE COMPOSITES," *Journal of Langmuir,* vol. 26, pp. 15302-15309, 2010.

[35] R.-H. Shi, Z.-R. Zhang, H.-L. Fan, T. Zhen, J. Shangguan, and J. Mi, "Cu-BASED METAL–ORGANIC FRAMEWORK/ACTIVATED CARBON COMPOSITES FOR SULFUR COMPOUNDS REMOVAL," *Journal of Applied Surface Science,* vol. 394, pp. 394-402, 2017.

DOI: 10.37200/IJPR/V24I2/PR200540
Received: 26 Dec 2019 | Revised: 10 Jan 2020 | Accepted: 21 Jan 2020

[36] S. J. Yang, J. H. Cho, K. S. Nahm, and C. R. Park, "ENHANCED HYDROGEN STORAGE CAPACITY OF Pt-LOADED CNT@MOF-5 HYBRID COMPOSITES," *International Journal Of Hydrogen Energy,* vol. 35, pp. 13062-13067, 2010.

[37] Z. Yu, J. Deschamps, L. Hamon, P. K. Prabhakaran, and P. Pré, "HYDROGEN ADSORPTION AND KINETICS IN MIL-101 (Cr) AND HYBRID ACTIVATED CARBON-MIL-101 (Cr) MATERIALS," *International Journal of Hydrogen Energy,* vol. 42, pp. 8021-8031, 2017.

[38] I. Ahmed and S. H. Jhung, "COMPOSITES OF METAL–ORGANIC FRAMEWORKS: PREPARATION AND APPLICATION IN ADSORPTION," *Journal of Materials Today,* vol. 17, pp. 136-146, 2014.

[39] L. Valenzano, B. Civalleri, S. Chavan, G. T. Palomino, C. O. Areán, and S. Bordiga, "COMPUTATIONAL AND EXPERIMENTAL STUDIES ON THE ADSORPTION OF CO, N_2, AND CO_2 ON Mg-MOF-74," *The Journal of Physical Chemistry C,* vol. 114, pp. 11185-11191, 2010.

[40] R. K. Nutor, X. Xu, X. Fan, S. Ren, X. He, and Y. Fang, "STRUCTURAL ANISOTROPY IN FeCuNbSiB ALLOYS: AN IN SITU SYNCHROTRON XRD STUDY," *Journal of Magnetism and Magnetic Materials,* vol. 454, pp. 51-56, 2018.

[41] S. Lawson, A. Hajari, A. A. Rownaghi, and F. Rezaei, "MOF IMMOBILIZATION ON THE SURFACE OF POLYMER-CORDIERITE COMPOSITE MONOLITHS THROUGH IN-SITU CRYSTAL GROWTH," *Separation and Purification Technology,* vol. 183, pp. 173-180, 2017.

[42] L. J. Wang, H. Deng, H. Furukawa, F. Gándara, K. E. Cordova, D. Peri, *et al.*, "SYNTHESIS AND CHARACTERIZATION OF METAL–ORGANIC FRAMEWORK-74 CONTAINING 2, 4, 6, 8, AND 10 DIFFERENT METALS," *Inorganic chemistry,* vol. 53, pp. 5881-5883, 2014.

[43] A. Yabuuchi, N. Oshima, B. O'Rourke, R. Suzuki, K. Ito, S. Sano, *et al.*, "STRUCTURAL AND DEFECT CHARACTERIZATION OF Gd-DOPED GaN FILMS BY X-RAY DIFFRACTION AND POSITRON ANNIHILATION," in *Journal of Physics: Conference Series*, 2014, p. 012023.

[44] B. H. Stuart, "ORGANIC MOLECULES," *Infrared Spectroscopy: Fundamentals And Applications,* pp. 71-93, 2004.

[45] N. Maksimchuk, M. Timofeeva, M. Melgunov, A. Shmakov, Y. A. Chesalov, D. Dybtsev, *et al.*, "HETEROGENEOUS SELECTIVE OXIDATION CATALYSTS BASED ON COORDINATION POLYMER MIL-101 AND TRANSITION METAL-SUBSTITUTED POLYOXOMETALATES," *Journal of Catalysis,* vol. 257, pp. 315-323, 2008.

DOI: 10.37200/IJPR/V24I2/PR200540
Received: 26 Dec 2019 | Revised: 10 Jan 2020 | Accepted: 21 Jan 2020